Accepted Manuscript

Title: Perspectives for Hyperpolarisation in Compact NMR

Author: Meghan E. Halse

PII: S0165-9936(15)30194-1
DOI: http://dx.doi.org/doi: 10.1016/j.trac.2016.05.004
Reference: TRAC 14747

To appear in: *Trends in Analytical Chemistry*

Please cite this article as: Meghan E. Halse, Perspectives for Hyperpolarisation in Compact NMR, *Trends in Analytical Chemistry* (2016), http://dx.doi.org/doi: 10.1016/j.trac.2016.05.004.

Perspectives for Hyperpolarisation in Compact NMR

Meghan E. Halse*

Department of Chemistry, University of York, Heslington York YO10 5DD UK

** Corresponding author: meghan.halse@york.ac.uk*

Highlights

- Hyperpolarisation techniques can significantly increase sensitivity of compact NMR.
- A range of promising hyperpolarization techniques are available.
- Promising applications include reaction monitoring and low-cost NMR/MRI.

Abstract

Nuclear magnetic resonance (NMR) is one of the most powerful analytical techniques currently available, with applications in fields ranging from synthetic chemistry to clinical diagnosis. Due to the size and cost of high-field spectrometers, NMR is generally considered to be ill-suited for industrial environments and field work. This conventional wisdom is currently being challenged through the development of NMR systems that are smaller, cheaper, more robust and portable. Despite remarkable progress in this area, potential applications are often limited by low sensitivity. Hyperpolarisation techniques have the potential to overcome this limitation and revolutionise the use of compact NMR. This review describes the state-of-the-art in NMR hyperpolarisation and presents promising examples of its application to compact NMR. Both the benefits and challenges associated with the different hyperpolarisation approaches are discussed and applications where these technologies have the potential to make a significant impact are highlighted.

Keywords: dynamic nuclear polarization (DNP); parahydrogen-induced polarization (PHIP); signal amplification by reversible exchange (SABRE); hyperpolarized gases; spin-exchange optical pumping (SEOP); low-field NMR

Abbreviations

CIDNP – chemically induced dynamic nuclear polarisation

DNP – dynamic nuclear polarisation

EF – Earth's magnetic field

ESR – electron spin resonance

MRI – magnetic resonance imaging

NMR – nuclear magnetic resonance

OE – Overhauser effect

p-H_2 – *para*hydrogen

PHIP – *para*hydrogen induced polarisation

ppb – parts per billion

ppm – parts per million

SABRE – signal amplification by reversible exchange

SEOP – spin-exchange optical pumping

SNR – signal-to-noise ratio

SPINOE – spin polarisation induced nuclear Overhauser effect

SQUID – super-conducting quantum interference device

1. Introduction

Nuclear Magnetic Resonance (NMR) spectroscopy and Magnetic Resonance Imaging (MRI) are powerful analytical tools with diverse applications across all of the physical and medical sciences. The power of NMR lies in the range of information available and its ability to probe structure and dynamics on length scales from the molecular to the macroscopic, and on timescales from picoseconds to days. While NMR benefits from a rich information content, it suffers from a low inherent sensitivity when compared to other standard analytical techniques such as mass spectrometry. The signal in an NMR experiment arises from a population imbalance across a set of nuclear spin states that are very close in energy relative to the available thermal energy at all temperatures above few mK. The energy difference is dominated by the Zeeman effect, whereby the spin angular momentum of a nucleus with a non-zero magnetic moment (i.e. with spin quantum number $I > 0$), is quantised along the axis of an external magnetic field, B_0. This quantisation leads to a set of $2I + 1$ possible nuclear spin states. Each energy level is associated with a quantum number m ($m \in \{-I, -I+1 \ldots I-1, I\}$) and has energy $E_m = -m\gamma\hbar B_0$, where the gyromagnetic ratio, γ, is a fundamental property of the nucleus and $\hbar$ is Plank's constant divided by 2π. The NMR signal is directly proportional to the normalised population difference between the Zeeman energy levels, also called the polarisation, *P*, which can be calculated for a given temperature, *T*, and field strength, B_0, using Boltzmann statistics. For spins with $I = ½$, such as protons (^{1}H) and ^{13}C, $P = \left(n_{\frac{1}{2}} - n_{-\frac{1}{2}}\right)/\left(n_{\frac{1}{2}} + n_{-\frac{1}{2}}\right) = \tanh(\gamma\hbar B_0/2kT)$, where $n_m = \exp(-E_m/kT)$ is the Boltzmann population of each energy level at thermal equilibrium. This corresponds to a polarisation of only 3 ppm/T for protons at 298 K (see Figure 1). The quest for improved sensitivity is one of the key driving forces for the move in modern NMR spectroscopy towards higher and higher fields, with 1 GHz (23.5 T) NMR spectrometers now available.[1, 2] While there are clear advantages to working in strong magnetic fields, the size and cost of these high-field NMR spectrometers render them unsuitable for many applications, particularly in industrial and other non-laboratory environments. Consequently, there has been a concerted effort in recent years to develop compact NMR systems that are sufficiently small, portable, and robust to be suitable for outside of the lab use.[3] These compact NMR instruments can be used to acquire high-resolution NMR spectra,[4] to measure bulk physical properties such as NMR relaxation and

molecular self-diffusion rates,[5] and to perform magnetic resonance imaging (MRI) experiments.[6] Example applications include: well logging and rock core analysis in the oil and gas industry,[7-9] *in situ* analysis of sea ice in Antarctica,[10] probing underground water aquifers,[11] quality control in the food industry,[5] non-destructive testing of cultural heritage artefacts,[12] and reaction monitoring and control.[4, 13, 14]

The term compact NMR encompasses a wide variety of NMR devices ranging in size from microcoils to benchtop instruments.[3] These devices can be broadly divided into two groups based on the strength of the magnetic field employed for NMR signal detection. In the first group are systems that operate in the field range of $0.04\ \mathrm{T} \leq B_0 \leq 2\ \mathrm{T}$ (^{1}H Larmor frequency of 2 - 85 MHz). These instruments are typically based on permanent magnets and can in some cases achieve a spectral resolution of 20 ppb.[4] This class of intermediate-field portable NMR devices includes high-resolution systems capable of measuring chemical shift and *J* coupling information, in a manner analogous to high-field laboratory devices,[4, 13] and lower-resolution systems, sometimes referred to as time-domain (TD) NMR spectrometers, that are used to measure NMR relaxation and molecular diffusion rates.[5] MRI experiments using permanent-magnet based compact devices are also possible.[6]

The second group of compact NMR devices operates below 0.04 T (< 2 MHz ^{1}H frequency) and typically employs either an electromagnet or the highly homogeneous Earth's magnetic field ($B_E \approx 50\ \mu\mathrm{T}$) for NMR signal detection. The incorporation of high-sensitivity detection methods, such as atomic magnetometers[15] or superconducting quantum interference devices (SQUIDs),[16] has expanded the range of NMR detection fields down to the so-called ultra-low field (B_0 < 50 μT)[17] and zero-field (B_0 < 1 nT) [18] regimes. While at the upper end of this range of NMR detection fields (B_0 ≥ 0.01 T) some chemical shift information can be extracted from the NMR spectra,[19] the key parameters measured with these instruments are *J* coupling constants (primarily heteronuclear), and NMR relaxation and molecular self-diffusion rates. This class of low-field NMR systems has also been used for MRI applications, where SQUID detectors provide sufficient sensitivity to achieve *in vivo* MRI in the microtesla regime.[20]

As discussed above, the Achilles heel of magnetic resonance is its low inherent sensitivity, a direct consequence of the low nuclear polarisation at thermal equilibrium. This challenge is particularly relevant to the case of compact NMR, where the detection fields are often much

lower than standard laboratory NMR spectrometers (see Figure 1b and Figure 1c). The NMR signal can be amplified by increasing the nuclear polarisation beyond that dictated by the Boltzmann distribution in the detection field. This approach is called hyperpolarisation and will be the focus of this review. The effectiveness of a given hyperpolarisation technique can be quantified either in terms of an enhancement factor or the level of polarisation. The enhancement factor is calculated as the ratio of the NMR signal observed with and without the use of hyperpolarisation under the given experimental conditions (e.g detection field and temperature). The polarisation is calculated as the product of the enhancement factor and the equilibrium nuclear polarisation at that detection field and temperature. Polarisation levels are often the most useful way to compare the efficiency of different hyperpolarisation methods because they are independent of the detection conditions. Therefore in this review, polarisation levels are quoted wherever possible.

It should be noted that NMR (and MRI) sensitivity also depends on the nuclear resonance frequency (the Larmor frequency, ω_0), which is linearly proportional to the detection field, B_0. The precise relationship between the observed signal-to-noise ratio (SNR) and the Larmor frequency depends on the method of detection. For the case of room temperature inductive detection where the dominant source of noise comes from the detection coil, NMR sensitivity is proportional to $(\omega_0)^{5/4}$. Interestingly, it has been shown that for hyperpolarised samples, the frequency dependence becomes $(\omega_0)^{1/2}$, indicating that hyperpolarisation methods have the potential to boost the sensitivity of compact NMR devices beyond that dictated by the polarisation level alone.[21]

The idea of hyperpolarisation dates back to the very early days of NMR, when Albert Overhauser recognised that the comparatively high polarisation of an unpaired electron, which arises due to its large gyromagnetic ratio ($\gamma_e/\gamma_{^1H} \approx 660$, see Figure 1), could be transferred to nearby NMR-active nuclei by saturating the electron spin resonance (ESR) transition of the conduction electrons in a metal.[22] His prediction was verified experimentally by Carver and Slichter, who observed NMR signal amplification for ^{7}Li nuclei in metallic lithium.[23] This hyperpolarisation method, called dynamic nuclear polarisation (DNP), remains one of the most effective NMR signal enhancement tools available today. For an interesting account of the history of DNP and the recent renaissance of this technique for biomedical applications, see the article by Slichter in *Reports on Progress in*

Physics.[24]

NMR and MRI signal amplification has been demonstrated for a wide range of nuclei (for example: ^{1}H, ^{3}He, ^{7}Li, ^{13}C, ^{15}N, ^{19}F, ^{31}P, ^{83}Kr and ^{129}Xe/^{131}Xe) using many different NMR hyperpolarisation methods including: brute-force polarisation,[25] variations on the original Overhauser DNP method, e.g. dissolution DNP (dDNP)[26] and magic-angle-spinning (MAS) DNP,[27] spin-exchange optical pumping of noble gas nuclei (SEOP),[28] *para*hydrogen induced polarisation (PHIP),[29, 30] signal amplification by reversible exchange (SABRE),[31] chemically induced dynamic nuclear polarisation (CIDNP),[32-34] and quantum-rotor induced polarisation.[35, 36] In each case, the spin polarisation of the target nuclei is enhanced through a transfer of spin order from another species and/or a rapid change in experimental conditions (i.e. field and/or temperature) between the polarisation and detection stages of the magnetic resonance experiment. Table 1 summarises the source of spin order and (if relevant) the polarisation transfer mechanism for each of the hyperpolarisation methods listed above.

One of the main driving forces behind the development of hyperpolarisation techniques has been for biomedical applications, particularly for the development of hyperpolarised contrast agents for *in vivo* MRI.[26, 37] See the recent review by Nikolaou *et al.* for an overview of the state-of-the-art in NMR hyperpolarisation techniques for biomedicine.[38] In solid-state NMR spectroscopy, hyperpolarisation has facilitated advances in areas such as the study of membrane proteins[39] and of pharmaceutical formulations at natural isotopic abundance.[40]

The translation of the many hyperpolarisation methods from a laboratory NMR or MRI instrument to a compact NMR device is conceptually straight-forward, particularly since many of the hyperpolarisation approaches physically separate the polarisation and detection phases of the experiment. In these cases, the compact NMR device can simply be substituted for the laboratory NMR or MRI instrument during signal detection. Indeed the use of a compact NMR device for signal detection often greatly simplifies the experimental set-up and can benefit from advantages such as the longer hyperpolarisation lifetimes at lower magnetic fields.[41] However, when designing a hyperpolarisation approach for compact NMR it is important to consider not only the NMR signal enhancements that can be achieved but also the impact that the hyperpolarisation method will have on the cost, size, complexity and portability of the instrument. In most cases a compromise must be made between the advantages of compact NMR (e.g. size and cost) and the level of sensitivity enhancement that is required. Therefore the choice of hyperpolarisation method is likely to be application specific. For example, in many biomedical applications higher cost instrumentation may be acceptable as long as the maximum polarisation levels (> 10%) are achieved. However, in industrial process monitoring it might be more advantageous to develop a technology that provides more modest signal enhancements (a couple orders of magnitude) while keeping the overall cost and complexity of the instrumentation low.

In this review, I focus on the hyperpolarisation techniques that have already shown promise for use with compact NMR. These include: brute-force hyperpolarisation, DNP, SEOP, PHIP, and SABRE. Examples in the literature where these methods have been combined with compact NMR to improve sensitivity will be highlighted. The benefits and challenges associated with these methods, as well as the applications where hyperpolarisation is most likely to have a significant impact in the field of compact NMR, will be discussed.

2. Hyperpolarisation in compact NMR

2.1 Brute-force Hyperpolarisation

One of the most commonly used signal enhancement methods in compact NMR, particularly where the detection field is very low (B_0 < 40 mT), is the so-called brute-force approach, where the polarisation of the NMR sample is carried out at a higher magnetic field strength, B_p, and/or a lower temperature than the detection stage of the experiment. Decoupling the polarisation and detection stages is advantageous because the polarisation field, B_p, need only be homogeneous to a few percent, while the detection field, B_0, requires field homogeneities on the order of ppm. In the brute-force approach, the pre-polarising field is often achieved by either switching on a crude electromagnet[10] or by placing the sample into a permanent magnet array.[18, 19, 42] The use of permanent magnets for pre-polarisation has the advantage of relatively high B_p field strengths (up to 2 T) and no duty-cycle limitations. However, the sample needs to be transported between the polarisation and detection fields. A pre-polarisation field generated electromagnetically is easily switched on and off. However, the fields that can be achieved with an electromagnet are typically limited to a few 10's of mT due resistive heating concerns. The relative advantages of pre-polarisation in a permanent magnet array (B_p = 300 mT) and an electromagnet (B_p = 18.7 mT) is illustrated by the Earth's field (EF) NMR spectra of water in Figure 2a. A 10 fold increase in signal-to-noise ratio (SNR) is observed for pre-polarisation in the 0.3 T permanent magnet array compared to the electromagnet. This is less than the predicted increase by a factor of 16 (the ratio of the two pre-polarisation fields) due to polarisation loss during sample transport in the case of the permanent magnet array.

The major advantage of brute-force polarisation is that no exogenous agent needs to be added to the sample, while the main limitation is that the signal enhancement scales linearly with the pre-polarisation field, B_p. Thus it is an attractive method for applications where the detection field is very low and doping the sample is not possible. For example, pre-polarisation with an electromagnet has been proposed for sensitivity enhancement in EF NMR measurements of subsurface water aquifers.[43]

Much higher enhancements can be achieved using the brute-force approach if the polarisation stage is carried out at a very low temperature. Hirsch *et al*. have demonstrated

that if pre-polarisation is carried out in a field of B_p = 14 T and at ~ 2.3 K, >0.1 % ^{13}C polarisation can be observed in small-molecule metabolites such at 1-^{13}C-acetic acid and 1-^{13}C-pyruvic acid, when the sample is rapidly heated and then detected at 1 T and 303 K.[25] While the observed polarisation levels are significant, the cost associated with this high-field/low-temperature instrumentation is likely to be incompatible with routine compact NMR applications. However, as will be discussed in more detail below, significant progress has been made recently in the storage and transport of hyperpolarised agents in the solid-state.[44] This work suggests that it may be possible to carry-out the generation of the hyperpolarised species offsite before transportation to the point of use, dramatically increasing the versatility and affordability of this technique.

2.2 Dynamic Nuclear Polarisation (DNP)

In a dynamic nuclear polarisation (DNP) experiment, the relatively high thermal polarisation of an unpaired electron is transferred to surrounding nuclei via irradiation at or near the ESR transition frequency of the electron. The mechanism that drives this polarisation transfer varies significantly depending on the experimental conditions, such as whether it is done in the solid or liquid state, and the source of the unpaired electrons.[46] For most applications, where no endogenous free radicals are present, a stable radical must be added to act as a source of hyperpolarisation. There are three main experimental approaches to DNP. In magic-angle spinning (MAS) DNP, the entire experiment is carried out in the solid-state at low temperature (< 150 K),[39] while Overhauser DNP experiments are performed in solution.[46] In dissolution DNP (dDNP), the polarisation stage occurs in the solid-state at very low temperatures (e.g. 1.2 K) and moderate field strengths (e.g. 3.4 T), where electron polarisation is near 100%. Once polarised at low temperature, the agent is rapidly dissolved and is either transferred into an NMR spectrometer for detection at ambient temperature[26] or injected into a patient inside an MRI scanner and subsequently imaged.[37]

In DNP the maximum achievable nuclear polarisation enhancement is the ratio of the electron and the nuclear polarisations under the given experimental conditions (i.e. field and temperature). In most cases, the maximum enhancement is simply the ratio of the electron and nuclear gyromagnetic ratios (~660 in the case of protons) and so at room temperature only modest polarisation levels can be achieved (see Figure 1). However, in dDNP the observed enhancements are much larger (e.g. 36% ^{13}C polarisation was observed

for an aqueous solution of [^{13}C]urea.[26]) This is because dDNP is in effect a combination of low-temperature brute-force hyperpolarisation of the electrons and subsequent polarisation transfer to the nuclei via DNP. Large polarisation enhancements are also possible for Overhauser DNP with nitroxide radicals in very low fields, where the ESR transition is dominated by the hyperfine interaction between the unpaired electron and the ^{14}N nucleus of the free radical. In this case, the electron polarisation is much larger than would be generated by the Zeeman interaction alone.[47-49] Nevertheless, the absolute level of ^{1}H polarisation remains quite low in this case (~1 ppm). In all DNP experiments, the maximum possible polarisation level is rarely observed in practice because the efficiency of the transfer from the electrons to the nuclei depends on many factors including: the extent of saturation of the electron transition, the size of the interaction between the unpaired electrons and the target nuclei, the mechanism of polarisation transfer, and the NMR relaxation properties of the system.[46] In many DNP applications, one of the key limiting factors is the saturation of the ESR transition, which is often quite broad. This issue becomes increasingly significant as the field (and hence the ESR transition frequency) increases. Efficient high-field, solid-state MAS DNP has only become feasible in recent years due to the work of Griffin and co-workers, who introduced gyrotrons as a source of high-powered microwaves at 100's of GHz (i.e. the Larmor frequency of electrons in high-field NMR spectrometers).[27] In liquids, the polarisation step of the DNP experiment is often carried out in a lower field, where saturation is possible, and then the sample is flowed into the high field for high-resolution detection.[50] Thus Overhauser DNP is an attractive method for compact NMR, where the low magnetic fields are a benefit rather than a limitation. In addition, liquid-state DNP is arguably the least demanding and costly to implement in terms of instrumentation because no cryogenic temperatures are required. However, room temperature Overhauser DNP cannot achieve the near-unity levels of polarisation that are accessible to the dDNP approach. Figure 2b presents a comparison of ^{1}H EF NMR spectra of water doped with 1.5 mM 4-oxy-tempo acquired using (top, grey) pre-polarisation at 18.7 mT, and (bottom, black) Overhauser DNP in a field of 2.5 mT (124 MHz ESR irradiation frequency). In this case, DNP provides a 14-fold SNR enhancement relative to that observed using brute-force polarisation, which corresponds to a ^{1}H polarisation level on the order of 1 ppm.

Overhauser DNP has been used for a number of applications in compact NMR including NMR and MRI in μT to mT fields,[49, 51-53] multi-dimensional Earth's field NMR spectroscopy,[48] field cycling relaxometry,[54] and indirect detection of ESR spectroscopy.[55, 56] By contrast, compact NMR instrumentation with MAS DNP capabilities is not currently available, despite the initial DNP experiments having been carried out at low field.[24] A compact NMR instrument equipped with a MAS probe for high-resolution solid-state NMR spectroscopy has recently been demonstrated by Sorensen *et al*.[57] Therefore, this is an area where significant growth could be seen in the coming years. A compact NMR device with MAS DNP capabilities could be particularly interesting for applications such as surface studies of materials and for structural studies of small molecules.[58] Dissolution DNP is a promising technique for the generation of hyperpolarised agents for a range of biomedical applications.[37, 38] The most significant limitation of dissolution DNP, as currently implemented, are cost and portability. As with the low-temperature, brute-force approach, substantial additional instrumentation is required and so it is not feasible to combine a compact NMR device with a dissolution DNP setup without significantly compromising both the affordability and complexity of the entire system. However methods for storing and transporting hyperpolarised agents in the solid-state[44, 59] may render dDNP a viable option in the future, even for applications where instrument cost and complexity are a significant concern.

2.3 Spin-exchange optical pumping (SEOP)

In a spin-exchange optical pumping (SEOP) experiment, the angular momentum of laser photons is transferred to the electrons of an alkali metal vapour (e.g. Rb) by exploiting the quantum mechanical selection rules for angular momentum.[28] The resultant high electron polarisation of the alkali metal vapour is transferred to nuclei of a noble gas (e.g. ^{3}He, ^{129}Xe, ^{131}Xe, or ^{83}Kr) through spin exchange collisions. The spin exchange is mediated by Fermi contact hyperfine interactions between the alkali electrons and noble gas nuclei.[28] In order to suppress the radiative decay of the excited electrons and to promote the transfer of polarisation to the noble gas nuclei, a partial pressure of a buffer gas, typically N_2, is added to the polarisation cell. Despite the fact that SEOP is limited to the hyperpolarisation of noble gas nuclei, it has many advantages. Specifically, near unity levels of polarisation can be achieved and, if isolated and stored properly, the hyperpolarisation of these gases can be

maintained for periods from hours to days.[28, 60] The ability to generate the hyperpolarisation offsite and then transport it to where it is to be used makes this an attractive method for compact NMR. Figure 2c presents a comparison of a ^{1}H EF NMR spectrum of toluene (pre-polarised at 18.7 mT) and a ^{129}Xe EF NMR spectrum of a 3% mixture of ^{129}Xe, hyperpolarised by SEOP to ~9%. Despite the very low Larmor frequency of ^{129}Xe in the Earth's field (756 Hz), very high resolution (<0.1 Hz) and SNR are achieved in the ^{129}Xe EF NMR spectrum.

The most prominent application of hyperpolarised gases is for *in vivo* MRI, particularly of the lungs.[61, 62] However, there are also many other applications, where the large chemical shift range of ^{129}Xe [63, 64] and the relaxation properties of the quadrupolar ^{83}Kr nucleus,[65] provide access to important chemical and structural information or where the hyperpolarised ^{129}Xe is used as a biosensor.[45] Hyperpolarised noble gases have been used in compact NMR for a range of applications including: MRI in the mT regime,[66-70] detection of ^{129}Xe chemical shifts in the Earth's magnetic field,[71] and NMR signal enhancement in μT to mT fields using the spin polarisation-induced nuclear Overhauser effect (SPINOE),[72] in which the noble gas hyperpolarisation is transferred to solvent nuclei through the nuclear Overhauser effect.[73] Beyond low-field *in vivo* imaging, hyperpolarised gases hold particular promise for compact NMR investigations of materials, where the chemical shift of ^{129}Xe and relaxation properties of ^{83}Kr can report on many important chemical and morphological features of the system.

2.4 Hyperpolarisation using parahydrogen: PHIP and SABRE

*Para*hydrogen (p-H_2) is the nuclear spin isomer of H_2 that contains a pair of protons that form a singlet spin state. This pure state has no magnetic moment and so p-H_2 does not give rise to a signal in a standard NMR experiment.[30] However, as first predicted by Bowers and Weitekamp in 1986, if a chemical reaction is used to place the two ^{1}H nuclei from p-H_2 into chemically and/or magnetically different environments in a product molecule, these former p-H_2 nuclei will produce highly enhanced NMR signals that are characteristic of the product that is formed.[29] This method is alternatively referred to as PASADENA (*para*hydrogen and synthesis allow dramatically enhanced nuclear alignment) or *para*hydrogen-induced polarisation (PHIP) and has been widely used in inorganic and organic chemistry to investigate hydrogenation reactions and for the detection of intermediates that are only present in very small quantities.[30] PHIP is also of significant interest as a method for generating hyperpolarised contrast agents for biomedical applications.[74-76] This can be

achieved using either the traditional hydrogenative PHIP approach[74-76] or the signal amplification by reversible exchange (SABRE)[31] method. In SABRE, a reversible exchange reaction involving *p*-H_2, a transition metal catalyst and the target substrate is used to catalytically transfer hyperpolarisation from *p*-H_2-derived protons to the substrate without the need for substrate hydrogenation. The ability to generate highly polarised species in solution, and without chemical alteration, has broadened the potential applications of *p*-H_2 hyperpolarisation, particularly in light of the fact that the reversibility of the exchange reaction means that continuous hyperpolarisation can be achieved.[77, 78]

Figure 3 demonstrates the use of SABRE hyperpolarisation for sensitivity enhancement of a high-resolution compact NMR spectrometer operating at 1.4 T (60 MHz) (Figure 3c). A comparison between the SABRE ^{1}H NMR spectra of 4-amino-pyridine acquired using a standard 400 MHz NMR spectrometer (Figure 3a) and the 60 MHz benchtop instrument (Figure 3b) illustrates that, while there is a loss of resolution due to the reduction in chemical shift dispersion when going from 9.4 T to 1.4 T, the single-scan SNR of the SABRE NMR spectra is similar for both instruments (^{1}H polarisation of ~ 1%) and there is sufficient resolution at 60 MHz to distinguish the proton resonances corresponding to substrate molecules in free solution and those bound to the polarisation transfer catalyst.

Both the original hydrogenative PHIP and the non-hydrogenative SABRE approaches have been used to sensitise compact NMR experiments for a range of applications. For example, PHIP and SABRE signals have been detected in liquid-state NMR spectroscopy in the zero-field regime,[80, 81] in the Earth's magnetic field,[82] in fields of 5-50 mT, [41, 83, 84] and in a field of 0.54 T using a time-domain NMR spectrometer.[85] PHIP and SABRE hyperpolarised liquids and gases have been imaged in mT fields,[84, 86, 87] and compact NMR instrumentation has been used to monitor the production of *p*-H_2 hyperpolarisation in fields of a few mT, where the SABRE polarisation transfer is the most efficient.[78, 88] In addition, the unique spin states generated by the *p*-H_2-based methodologies have been exploited to provide chemical speciation information in mT fields that would otherwise be absent due to limited chemical shift resolution.[89, 90]

There are many advantages of *para*hydrogen hyperpolarisation. First, generating *p*-H_2 is relatively cheap and easy. At room temperature only 25% of H_2 is the in *para* form, while the remaining 75% is *ortho*hydrogen, the nuclear triplet spin isomer of H_2. The proportion of

p-H_2 can be increased by cooling H_2 gas in the presence of a catalyst that promotes conversion between the *para* and *ortho* forms. At liquid nitrogen temperatures (77 K), H_2 contains 50% *p*-H_2 at thermal equilibrium, while at 20 K, the proportion of *p*-H_2 increases to > 99.9%.[91] In the absence of a catalyst, the *para* to *ortho* conversion is very slow. Therefore, once enriched at low temperature, the *p*-H_2 gas can be heated to room temperature and stored for periods from hours to days.[30] Therefore *p*-H_2 can be generated off-site, stored and then transported to the point of use. Other advantages of *p*-H_2 hyperpolarisation include the large polarisation levels that can be achieved (10% ^{1}H polarisation[92] and ^{15}N polarisation[93] have been reported), the rapid build-up of polarisation, which can be on the order of seconds, and the ability to generate continuous polarisation.[77] The main challenge associated with PHIP and SABRE is the need for a chemical reaction to unlock the *p*-H_2-derived hyperpolarisation. In the PHIP case, an unsaturated precursor and a hydrogenation catalyst is required. In the SABRE case a transition metal catalyst needs to be added to mediate the polarisation transfer from *p*-H_2 to the substrate. The nuclear spin states that result from *p*-H_2 hyperpolarisation are more complex than for NMR polarisation at thermal equilibrium. This is both a challenge and an opportunity. The difficulty arises from the fact that *p*-H_2-derived ^{1}H NMR signals often have an anti-phase character, which can lead to significant signal cancellation if resonances are not well resolved. The advantage is due to the fact that these unique spin states can be manipulated to provide additional chemical information about the hyperpolarised molecules and can be transferred to other more slowly-relaxing nuclei (e.g. ^{13}C) or into long-lived nuclear spin states[94] for storage and later detection. Promising applications of *p*-H_2 hyperpolarisation in compact NMR include the generation of highly polarised species for μT to mT MRI, with potential applications for medical diagnosis using a low-cost MRI device, and for reaction monitoring and control, where *p*-H_2 hyperpolarisation could be used to track the progress of a reaction and also to detect species present at low concentration.

4. Conclusions and Future Outlook

Hyperpolarisation has been successfully combined with compact NMR devices with fields ranging from < 1 nT up to 2 T to achieve maximum polarisation levels on the order of 10% for a range of nuclei, e.g. ^{1}H, ^{13}C, ^{15}N, ^{19}F, and ^{129}Xe. While these experiments demonstrate the potential of hyperpolarisation to sensitise compact NMR and MRI, there remain several

challenges, both with regards to the hyperpolarisation techniques themselves and their integration with compact NMR.

One of the advantages of NMR spectroscopy as an analytical technique, particularly for reaction monitoring, is that peak integrals can be analysed to obtain quantitative information regarding the relative concentrations of species in solution. In hyperpolarised NMR, the level of observed NMR signal may not vary with concentration in the same way for all species due to factors such as polarisation transfer efficiency and NMR relaxation. Establishing that hyperpolarised NMR can produce quantitative information regarding the relative concentration of species in solution will be a key step to unlocking applications such as process control and reaction monitoring.

Another important consideration is the lifetime of the hyperpolarisation. By definition, hyperpolarisation is a non-equilibrium distribution of nuclear spin populations and therefore the system will return to equilibrium via NMR relaxation. In order to use hyperpolarisation to improve NMR sensitivity it is important to consider not only the extent to which the nuclear spins can be polarised but also the lifetime of this hyperpolarisation. It should be noted that in the SABRE approach an equilibrium can be reached where a continuous level of polarisation is maintained. [77, 78] However, the maximum polarisation that can be achieved in this continuous mode will depend on the hyperpolarisation lifetime as well as the efficiency of the underlying hyperpolarisation process. One benefit of compact NMR is that hyperpolarisation lifetimes are often longer at lower magnetic fields (i.e. at 1 T vs. 9.4 T). Nevertheless, there would be significant benefits to extending hyperpolarisation lifetimes from the order of seconds to minutes or even hours. One potential approach lies in the generation of so-called long-lived states (LLS), whose lifetimes can reach 10's of minutes due to the symmetry properties of the spin system.[95] One example of this approach in high-field NMR is the use of a hyperpolarised LLS, generated using dDNP, for detecting ligand binding in drug screening applications.[21]

The cost and complexity of hyperpolarisation instrumentation is another challenge that needs to be considered. One potential solution is to generate hyperpolarised agents offsite and then to transport these species to the point of use. While this is a well-known feature of hyperpolarised gases (e.g. ^{129}Xe and *p*-H_2), recent reports suggest that storage and transport should also be possible for hyperpolarised agents in the solid state. In a recent meeting on

hyperpolarisation in the Netherlands, Sami Jannin (EPFL, Switzerland) discussed the potential for the storage and transportation of species hyperpolarised by dDNP, demonstrating a remarkable lifetime for hyperpolarised 1-^{13}C-pyruvate of 29 hours when stored at 4.2 K and 6.7 T.[59] Hirsch *et al.* have also demonstrated the transportation of brute-force hyperpolarised agents with transfer times ranging from 5 minutes to 5 hours, depending on the storage field and temperature.[44] If these ideas prove to be generally applicable, it would revolutionise the way we think about hyperpolarisation and compact NMR, not only for species hyperpolarised by dissolution DNP and low-temperature brute-force methods but by the other approaches as well.

In conclusion, NMR hyperpolarisation presents an exciting opportunity to address one of the most significant challenges associated with compact NMR: low sensitivity. Currently available technologies, including brute-force hyperpolarisation, DNP, SEOP, PHIP, and SABRE, have been used with a wide range of compact NMR instruments to nuclear polarisation levels on the order of 10's of percent for a range of difference nuclei. Promising applications include low cost NMR and MRI, compact MRI for biomedical applications using hyperpolarised contrast agents and benchtop instrumentation for the characterisation of porous materials and for reaction monitoring and control. It is important to note that hyperpolarisation in NMR continues to be a dynamic field of research, with several of the major breakthroughs highlighted in this review (e.g. dissolution DNP and SABRE) having been made within the last 10-15 years. New developments in instrumentation and methods for both the generation and storage of hyperpolarisation will only further advance the goal of developing truly low-cost, high-sensitivity, portable NMR and MRI devices suitable for a wide range of real-world applications.

5. Acknowledgements

I am grateful to the EPSRC for financial support (grant EP/M020983/1) and I would like to thank Peter Richardson for providing the SABRE hyperpolarisation data. I would also like to thank Simon Duckett, Robin Perutz, and Alison Nordon for helpful discussions.

6. References

1. A. Bhattacharya, Chemistry: Breaking the Billion-Hertz Barrier, *Nature* **463**, 605 (2010).

2. K. Hashi, S. Ohki, S. Matsumoto, G. Nishijima, A. Goto, K. Deguchi, K. Yamada, T. Noguchi, S. Sakai, M. Takahashi, Y. Yanagisawa, S. Iguchi, T. Yamazaki, H. Maeda, R. Tanaka, T. Nemoto, H. Suematsu, T. Miki, K. Saito, T. Shimizu, Achievement of 1020 MHz NMR, *Journal of Magnetic Resonance* **256**, 30 (2015).
3. S. S. Zalesskiy, E. Danieli, B. Bluemich, V. P. Ananikov, Miniaturization of NMR Systems: Desktop Spectrometers, Microcoil Spectroscopy, and "NMR on a Chip" for Chemistry, Biochemistry, and Industry, *Chemical Reviews* **114**, 5641 (2014).
4. E. Danieli, J. Perlo, A. L. L. Duchateau, G. K. M. Verzijl, V. M. Litvinov, B. Blumich, F. Casanova, On-Line Monitoring of Chemical Reactions by Using Bench-Top Nuclear Magnetic Resonance Spectroscopy, *Chemphyschem* **15**, 3060 (2014).
5. J. van Duynhoven, A. Voda, M. Witek, H. Van As, Time-Domain NMR Applied to Food Products in *Annual Reports on NMR Spectroscopy, Vol 69,* G. A. Webb, Ed. (2010), vol. 69, pp. 145-197.
6. J. Perlo, E. V. Silletta, E. Danieli, G. Cattaneo, R. H. Acosta, B. Bluemich, F. Casanova, Desktop MRI as a Promising Tool for Mapping Intra-Aneurismal Flow, *Magnetic Resonance Imaging* **33**, 328 (2015).
7. Y. Q. Song, Magnetic Resonance of Porous Media (Mrpm): A Perspective, *Journal of Magnetic Resonance* **229**, 12 (2013).
8. R. J. S. Brown, R. Chandler, J. A. Jackson, R. L. Kleinberg, M. N. Miller, Z. Paltiel, M. G. Prammer, History of NMR Well Logging, *Concepts in Magnetic Resonance* **13**, 335 (2001).
9. B. Blumich, J. Mauler, A. Haber, J. Perlo, E. Danieli, F. Casanova, Mobile NMR for Geophysical Analysis and Materials Testing, *Petroleum Science* **6**, 1 (2009).
10. P. T. Callaghan, A. Coy, R. Dykstra, C. A. Eccles, M. E. Halse, M. W. Hunter, O. R. Mercier, J. N. Robinson, New Zealand Developments in Earth's Field NMR, *Applied Magnetic Resonance* **32**, 63 (2007).
11. O. A. Shushakov, Groundwater NMR in Conductive Water, *Geophysics* **61**, 998 (1996).
12. B. Blumich, F. Casanova, J. Perlo, F. Presciutti, C. Anselmi, B. Doherty, Noninvasive Testing of Art and Cultural Heritage by Mobile NMR, *Accounts of Chemical Research* **43**, 761 (2010).
13. V. Sans, L. Porwol, V. Dragone, L. Cronin, A Self Optimizing Synthetic Organic Reactor System Using Real-Time in-Line NMR Spectroscopy, *Chemical Science* **6**, 1258 (2015).
14. F. D. de Andrade, L. A. Colnago, Use of NMR as an Online Sensor in Industrial Processes, *Quimica Nova* **35**, 2019 (2012).
15. D. Budker, M. Romalis, Optical Magnetometry, *Nature Physics* **3**, 227 (2007).
16. J. Clarke, M. Hatridge, M. Mossle, SQUID-Detected Magnetic Resonance Imaging in Microtesla Fields in *Annual Review of Biomedical Engineering*. (2007), vol. 9, pp. 389-413.
17. R. McDermott, A. H. Trabesinger, M. Muck, E. L. Hahn, A. Pines, J. Clarke, Liquid-State NMR and Scalar Couplings in Microtesla Magnetic Fields, *Science* **295**, 2247 (2002).
18. M. P. Ledbetter, T. Theis, J. W. Blanchard, H. Ring, P. Ganssle, S. Appelt, B. Bluemich, A. Pines, D. Budker, Near-Zero-Field Nuclear Magnetic Resonance, *Physical Review Letters* **107**, 107601 (2011).
19. S. Appelt, S. Gloggler, F. W. Hasing, U. Sieling, A. G. Nejad, B. Blumich, NMR Spectroscopy in the Milli-Tesla Regime: Measurement of H-1 Chemical-Shift Differences Below the Line Width, *Chemical Physics Letters* **485**, 217 (2010).

20. B. Inglis, K. Buckenmaier, P. SanGiorgio, A. F. Pedersen, M. A. Nichols, J. Clarke, MRI of the Human Brain at 130 Microtesla, *Proceedings of the National Academy of Sciences of the United States of America* **110**, 19194 (2013).
21. A. M. Coffey, M. L. Truong, E. Y. Chekmenev, Low-Field MRI Can Be More Sensitive Than High-Field MRI, *Journal of Magnetic Resonance* **237**, 169 (2013).
22. A. W. Overhauser, Polarization of Nuclei in Metals, *Physical Review* **92**, 411 (1953).
23. T. R. Carver, C. P. Slichter, Polarization of Nuclear Spins in Metals, *Physical Review* **92**, 212 (1953).
24. C. P. Slichter, The Discovery and Renaissance of Dynamic Nuclear Polarization, *Reports on Progress in Physics* **77**, 072501 (2014).
25. M. L. Hirsch, N. Kalechofsky, A. Belzer, M. Rosay, J. G. Kempf, Brute-Force Hyperpolarization for NMR and MRI, *Journal of the American Chemical Society* **137**, 8428 (2015).
26. J. H. Ardenkjaer-Larsen, B. Fridlund, A. Gram, G. Hansson, L. Hansson, M. H. Lerche, R. Servin, M. Thaning, K. Golman, Increase in Signal-to-Noise Ratio of > 10,000 Times in Liquid-State NMR, *Proceedings of the National Academy of Sciences of the United States of America* **100**, 10158 (2003).
27. L. R. Becerra, G. J. Gerfen, R. J. Temkin, D. J. Singel, R. G. Griffin, Dynamic Nuclear-Polarization with a Cyclotron-Resonance Maser at 5-T, *Physical Review Letters* **71**, 3561 (1993).
28. B. M. Goodson, Nuclear Magnetic Resonance of Laser-Polarized Noble Gases in Molecules, Materials, and Organisms, *Journal of Magnetic Resonance* **155**, 157 (2002).
29. C. R. Bowers, D. P. Weitekamp, Transformation of Symmetrization Order to Nuclear-Spin Magnetization by Chemical-Reaction and Nuclear-Magnetic-Resonance, *Physical Review Letters* **57**, 2645 (1986).
30. R. A. Green, R. W. Adams, S. B. Duckett, R. E. Mewis, D. C. Williamson, G. G. R. Green, The Theory and Practice of Hyperpolarization in Magnetic Resonance Using Parahydrogen, *Progress in Nuclear Magnetic Resonance Spectroscopy* **67**, 1 (2012).
31. R. W. Adams, J. A. Aguilar, K. D. Atkinson, M. J. Cowley, P. I. P. Elliott, S. B. Duckett, G. G. R. Green, I. G. Khazal, J. Lopez-Serrano, D. C. Williamson, Reversible Interactions with Para-Hydrogen Enhance NMR Sensitivity by Polarization Transfer, *Science* **323**, 1708 (2009).
32. J. Bargon, H. Fischer, Kernresonanz-Emissionslinien Wahrend Rascher Radikalreaktionen .2. Chemisch Induzierte Dynamische Kernpolarisation, *Zeitschrift Fur Naturforschung Part a-Astrophysik Physik Und Physikalische Chemie* **A 22**, 1556 (1967).
33. R. G. Lawler, Chemically Induced Dynamic Nuclear Polarization, *Journal of the American Chemical Society* **89**, 5519 (1967).
34. M. Goez, Photo-CIDNP Spectroscopy in *Annual Reports on NMR Spectroscopy, Vol 66,* G. A. Webb, Ed. (2009), vol. 66, pp. 77-147.
35. B. Meier, J.-N. Dumez, G. Stevanato, J. T. Hill-Cousins, S. S. Roy, P. Hakansson, S. Mamone, R. C. D. Brown, G. Pileio, M. H. Levitt, Long-Lived Nuclear Spin States in Methyl Groups and Quantum-Rotor-Induced Polarization, *Journal of the American Chemical Society* **135**, 18746 (2013).
36. C. Ludwig, M. Saunders, I. Marin-Montesinos, U. L. Guenther, Quantum Rotor Induced Hyperpolarization, *Proceedings of the National Academy of Sciences of the*

United States of America **107**, 10799 (2010).

37. S. J. Nelson, J. Kurhanewicz, D. B. Vigneron, P. E. Z. Larson, A. L. Harzstark, M. Ferrone, M. van Criekinge, J. W. Chang, R. Bok, I. Park, G. Reed, L. Carvajal, E. J. Small, P. Munster, V. K. Weinberg, J. H. Ardenkjaer-Larsen, A. P. Chen, R. E. Hurd, L. I. Odegardstuen, F. J. Robb, J. Tropp, J. A. Murray, Metabolic Imaging of Patients with Prostate Cancer Using Hyperpolarized 1-C-13 Pyruvate, *Science Translational Medicine* **5**, 198ra108 (2013).
38. P. Nikolaou, B. M. Goodson, E. Y. Chekmenev, NMR Hyperpolarization Techniques for Biomedicine, *Chemistry-a European Journal* **21**, 3156 (2015).
39. Q. Z. Ni, E. Daviso, T. V. Can, E. Markhasin, S. K. Jawla, T. M. Swager, R. J. Temkin, J. Herzfeld, R. G. Griffin, High Frequency Dynamic Nuclear Polarization, *Accounts of Chemical Research* **46**, 1933 (2013).
40. A. J. Rossini, C. M. Widdifield, A. Zagdoun, M. Lelli, M. Schwarzwaelder, C. Coperet, A. Lesage, L. Emsley, Dynamic Nuclear Polarization Enhanced NMR Spectroscopy for Pharmaceutical Formulations, *Journal of the American Chemical Society* **136**, 2324 (2014).
41. K. W. Waddell, A. M. Coffey, E. Y. Chekmenev, In Situ Detection of PHIP at 48 Mt: Demonstration Using a Centrally Controlled Polarizer, *Journal of the American Chemical Society* **133**, 97 (2011).
42. S. Gloggler, B. Blumich, S. Appelt, NMR Spectroscopy for Chemical Analysis at Low Magnetic Fields in *Modern NMR Methodology,* H. Heise, S. Matthews, Eds. (2013), vol. 335, pp. 1-22.
43. G. de Pasquale, O. Mohnke, Numerical Study of Prepolarized Surface Nuclear Magnetic Resonance in the Vadose Zone, *Vadose Zone Journal* **13**, (2014).
44. M. L. Hirsch, B. A. Smith, M. Mattingly, A. G. Goloshevsky, M. Rosay, J. G. Kempf, Transport and Imaging of Brute-Force C-13 Hyperpolarization, *Journal of Magnetic Resonance* **261**, 87 (2015).
45. L. Schroder, T. J. Lowery, C. Hilty, D. E. Wemmer, A. Pines, Molecular Imaging Using a Targeted Magnetic Resonance Hyperpolarized Biosensor, *Science* **314**, 446 (2006).
46. U. L. Guenther, Dynamic Nuclear Hyperpolarization in Liquids in *Modern NMR Methodology,* H. Heise, S. Matthews, Eds. (2013), vol. 335, pp. 23-69.
47. T. Guiberteau, D. Grucker, Dynamic Nuclear-Polarization of Water Protons by Saturation of Sigma and Pi EPR Transitions of Nitroxides, *Journal of Magnetic Resonance Series A* **105**, 98 (1993).
48. M. E. Halse, P. T. Callaghan, A Dynamic Nuclear Polarization Strategy for Multi-Dimensional Earth's Field NMR Spectroscopy, *Journal of Magnetic Resonance* **195**, 162 (2008).
49. S.-J. Lee, J. H. Shim, K. Kim, K. K. Yu, S.-m. Hwang, Dynamic Nuclear Polarization in the Hyperfine-Field-Dominant Region, *Journal of Magnetic Resonance* **255**, 114 (2015).
50. S. E. Korchak, A. S. Kiryutin, K. L. Ivanov, A. V. Yurkovskaya, Y. A. Grishin, H. Zimmermann, H. M. Vieth, Low-Field, Time-Resolved Dynamic Nuclear Polarization with Field Cycling and High-Resolution NMR Detection, *Applied Magnetic Resonance* **37**, 515 (2010).
51. V. S. Zotev, T. Owens, A. N. Matlashov, I. M. Savukov, J. J. Gomez, M. A. Espy, Microtesla MRI with Dynamic Nuclear Polarization, *Journal of Magnetic Resonance* **207**, 78 (2010).

52. S.-J. Lee, K. Kim, C. S. Kang, S.-m. Hwang, Y.-H. Lee, Pre-Polarization Enhancement by Dynamic Nuclear Polarization in SQUID-Based Ultra-Low-Field Nuclear Magnetic Resonance, *Superconductor Science & Technology* **23**, 115008 (2010).
53. M. D. Lingwood, I. A. Ivanov, A. R. Cote, S. Han, Heisenberg Spin Exchange Effects of Nitroxide Radicals on Overhauser Dynamic Nuclear Polarization in the Low Field Limit at 1.5 Mt, *Journal of Magnetic Resonance* **204**, 56 (2010).
54. O. Neudert, C. Mattea, S. Stapf, M. Reh, H. W. Spiess, K. Muennemann, Fast-Field-Cycling Relaxometry Enhanced by Dynamic Nuclear Polarization, *Microporous and Mesoporous Materials* **205**, 70 (2015).
55. D. J. Lurie, I. Nicholson, J. R. Mallard, Low-Field EPR Measurements by Field-Cycled Dynamic Nuclear-Polarization, *Journal of Magnetic Resonance* **95**, 405 (1991).
56. T. Guiberteau, D. Grucker, EPR Spectroscopy by Dynamic Nuclear Polarization in Low Magnetic Field, *Journal of Magnetic Resonance Series B* **110**, 47 (1996).
57. M. K. Sorensen, O. Bakharev, O. Jensen, H. J. Jakobsen, J. Skibsted, N. C. Nielsen, Magic-Angle Spinning Solid-State Multinuclear NMR on Low-Field Instrumentation, *Journal of Magnetic Resonance* **238**, 20 (2014).
58. A. J. Rossini, A. Zagdoun, M. Lelli, A. Lesage, C. Coperet, L. Emsley, Dynamic Nuclear Polarization Surface Enhanced NMR Spectroscopy, *Accounts of Chemical Research* **46**, 1942 (2013).
59. S. Jannin, Hybrid Polarising Solids for Pure Hyperpolarised Liquids through Dissolution Dynamic Nuclear Polarisation, presented at the Hyperpolarised Magnetic Resonance Conference, Egmond Aan Zee, The Netherlands, 2015.
60. P. Nikolaou, A. M. Coffey, L. L. Walkup, B. M. Gust, N. Whiting, H. Newton, S. Barcus, I. Muradyan, M. Dabaghyan, G. D. Moroz, M. S. Rosen, S. Patz, M. J. Barlow, E. Y. Chekmenev, B. M. Goodson, Near-Unity Nuclear Polarization with an Open-Source Xe-129 Hyperpolarizer for NMR and MRI, *Proceedings of the National Academy of Sciences of the United States of America* **110**, 14150 (2013).
61. D. M. L. Lilburn, G. E. Pavlovskaya, T. Meersmann, Perspectives of Hyperpolarized Noble Gas MRI Beyond He-3, *Journal of Magnetic Resonance* **229**, 173 (2013).
62. K. Ruppert, Biomedical Imaging with Hyperpolarized Noble Gases, *Reports on Progress in Physics* **77**, 116701 (2014).
63. D. Raftery, Xenon NMR Spectroscopy in *Annual Reports on NMR Spectroscopy, Vol 57,* G. A. Webb, Ed. (Elsevier Academic Press Inc, San Diego, 2006), vol. 57, pp. 205-270.
64. K. V. Romanenko, Xe-129 NMR Studies of Xenon Adsorption in *Annual Reports on NMR Spectroscopy, Vol 69,* G. A. Webb, Ed. (2010), vol. 69, pp. 1.
65. Z. I. Cleveland, T. Meersmann, Studying Porous Materials with Krypton-83 NMR Spectroscopy, *Magnetic Resonance in Chemistry* **45**, S12 (2007).
66. K. Safiullin, C. Talbot, P.-J. Nacher, Achieving High Spatial Resolution and High SNR in Low-Field MRI of Hyperpolarised Gases with Slow Low Angle Shot, *Journal of Magnetic Resonance* **227**, 72 (2013).
67. L. L. Tsai, R. W. Mair, M. S. Rosen, S. Patz, R. L. Walsworth, An Open-Access, Very-Low-Field MRI System for Posture-Dependent He-3 Human Lung Imaging, *Journal of Magnetic Resonance* **193**, 274 (2008).
68. C. H. Tseng, G. P. Wong, V. R. Pomeroy, R. W. Mair, D. P. Hinton, D. Hoffmann, R. E. Stoner, F. W. Hersman, D. G. Cory, R. L. Walsworth, Low-Field MRI of Laser Polarized Noble Gas, *Physical Review Letters* **81**, 3785 (1998).

69. A. Wong-Foy, S. Saxena, A. J. Moule, H. M. L. Bitter, J. A. Seeley, R. McDermott, J. Clarke, A. Pines, Laser-Polarized Xe-129 NMR and MRI at Ultralow Magnetic Fields, *Journal of Magnetic Resonance* **157**, 235 (2002).
70. Y. Zheng, G. D. Cates, W. A. Tobias, J. P. Mugler, G. W. Miller, Very-Low-Field MRI of Laser Polarized Xenon-129, *Journal of Magnetic Resonance* **249**, 108 (2014).
71. S. Appelt, F. W. Hasing, H. Kuhn, J. Perlo, B. Blumich, Mobile High Resolution Xenon Nuclear Magnetic Resonance Spectroscopy in the Earth's Magnetic Field, *Physical Review Letters* **94**, 197602 (2005).
72. G. Navon, Y. Q. Song, T. Room, S. Appelt, R. E. Taylor, A. Pines, Enhancement of Solution NMR and MRI with Laser-Polarized Xenon, *Science* **271**, 1848 (1996).
73. S. Appelt, F. W. Haesing, S. Baer-Lang, N. J. Shah, B. Blumich, Proton Magnetization Enhancement of Solvents with Hyperpolarized Xenon in Very Low-Magnetic Fields, *Chemical Physics Letters* **348**, 263 (2001).
74. E. Y. Chekmenev, J. Hoevener, V. A. Norton, K. Harris, L. S. Batchelder, P. Bhattacharya, B. D. Ross, D. P. Weitekamp, Pasadena Hyperpolarization of Succinic Acid for MRI and NMR Spectroscopy, *Journal of the American Chemical Society* **130**, 4212 (2008).
75. M. Goldman, H. Johannesson, O. Axelsson, M. Karlsson, Hyperpolarization of C-13 through Order Transfer from Parahydrogen: A New Contrast Agent for Mfi, *Magnetic Resonance Imaging* **23**, 153 (2005).
76. J.-B. Hoevener, E. Y. Chekmenev, K. C. Harris, W. H. Perman, L. W. Robertson, B. D. Ross, P. Bhattacharya, Pasadena Hyperpolarization of C-13 Biomolecules: Equipment Design and Installation, *Magnetic Resonance Materials in Physics Biology and Medicine* **22**, 111 (2009).
77. J.-B. Hoevener, S. Knecht, N. Schwaderlapp, J. Hennig, D. von Elverfeldt, Continuous Re-Hyperpolarization of Nuclear Spins Using Parahydrogen: Theory and Experiment, *Chemphyschem* **15**, 2451 (2014).
78. J.-B. Hoevener, N. Schwaderlapp, T. Lickert, S. B. Duckett, R. E. Mewis, L. A. R. Highton, S. M. Kenny, G. G. R. Green, D. Leibfritz, J. G. Korvink, J. Hennig, D. von Elverfeldt, A Hyperpolarized Equilibrium for Magnetic Resonance, *Nature Communications* **4**, 2946 (2013).
79. K. M. Appleby, R. E. Mewis, A. M. Olaru, G. G. R. Green, I. J. S. Fairlamb, S. B. Duckett, Investigating Pyridazine and Phthalazine Exchange in a Series of Iridium Complexes in Order to Define Their Role in the Catalytic Transfer of Magnetisation from Para-Hydrogen, *Chemical Science* **6**, 3981 (2015).
80. T. Theis, P. Ganssle, G. Kervern, S. Knappe, J. Kitching, M. P. Ledbetter, D. Budker, A. Pines, Parahydrogen-Enhanced Zero-Field Nuclear Magnetic Resonance, *Nature Physics* **7**, 571 (2011).
81. T. Theis, M. P. Ledbetter, G. Kervern, J. W. Blanchard, P. J. Ganssle, M. C. Butler, H. D. Shin, D. Budker, A. Pines, Zero-Field NMR Enhanced by Parahydrogen in Reversible Exchange, *Journal of the American Chemical Society* **134**, 3987 (2012).
82. B. C. Hamans, A. Andreychenko, A. Heerschap, S. S. Wijmenga, M. Tessari, NMR at Earth's Magnetic Field Using Para-Hydrogen Induced Polarization, *Journal of Magnetic Resonance* **212**, 224 (2011).
83. Q. Gong, A. Gordji-Nejad, B. Bluemich, S. Appelt, Trace Analysis by Low-Field NMR: Breaking the Sensitivity Limit, *Analytical Chemistry* **82**, 7078 (2010).
84. D. A. Barskiy, K. V. Kovtunov, I. V. Koptyug, P. He, K. A. Groome, Q. A. Best, F. Shi, B.

M. Goodson, R. V. Shchepin, M. L. Truong, A. M. Coffey, K. W. Waddell, E. Y. Chekmenev, In Situ and Ex Situ Low-Field NMR Spectroscopy and MRI Endowed by SABRE Hyperpolarization, *Chemphyschem* **15**, 4100 (2014).

85. T. Ratajczyk, T. Gutmann, S. Dillenberger, S. Abdulhussaein, J. Frydel, H. Breitzke, U. Bommerich, T. Trantzschel, J. Bernarding, P. C. M. M. Magusin, G. Buntkowsky, Time Domain Para Hydrogen Induced Polarization, *Solid State Nuclear Magnetic Resonance* **43-44**, 14 (2012).
86. A. M. Coffey, K. V. Kovtunov, D. A. Barskiy, I. V. Koptyug, R. V. Shchepin, K. W. Waddell, P. He, K. A. Groome, Q. A. Best, F. Shi, B. M. Goodson, E. Y. Chekmenev, High-Resolution Low-Field Molecular Magnetic Resonance Imaging of Hyperpolarized Liquids, *Analytical Chemistry* **86**, 9042 (2014).
87. K. V. Kovtunov, M. L. Truong, D. A. Barskiy, I. V. Koptyug, A. M. Coffey, K. W. Waddell, E. Y. Chekmenev, Long-Lived Spin States for Low-Field Hyperpolarized Gas MRI, *Chemistry-a European Journal* **20**, 14629 (2014).
88. R. Borowiak, N. Schwaderlapp, F. Huethe, T. Lickert, E. Fischer, S. Baer, J. Hennig, D. von Elverfeldt, J.-B. Hoevener, A Battery-Driven, Low-Field NMR Unit for Thermally and Hyperpolarized Samples, *Magnetic Resonance Materials in Physics Biology and Medicine* **26**, 491 (2013).
89. J. Colell, P. Tuerschmann, S. Gloeggler, P. Schleker, T. Theis, M. Ledbetter, D. Budker, A. Pines, B. Bluemich, S. Appelt, Fundamental Aspects of Parahydrogen Enhanced Low-Field Nuclear Magnetic Resonance, *Physical Review Letters* **110**, 137602 (2013).
90. I. Prina, L. Buljubasich, R. H. Acosta, Parahydrogen Discriminated PHIP at Low Magnetic Fields, *Journal of Magnetic Resonance* **251**, 1 (2015).
91. B. B. Feng, A. M. Coffey, R. D. Colon, E. Y. Chekmenev, K. W. Waddell, A Pulsed Injection Parahydrogen Generator and Techniques for Quantifying Enrichment, *Journal of Magnetic Resonance* **214**, 258 (2012).
92. M. J. Cowley, R. W. Adams, K. D. Atkinson, M. C. R. Cockett, S. B. Duckett, G. G. R. Green, J. A. B. Lohman, R. Kerssebaum, D. Kilgour, R. E. Mewis, Iridium N-Heterocyclic Carbene Complexes as Efficient Catalysts for Magnetization Transfer from Para-Hydrogen, *Journal of the American Chemical Society* **133**, 6134 (2011).
93. T. Theis, M. L. Truong, A. M. Coffey, R. V. Shchepin, K. W. Waddell, F. Shi, B. M. Goodson, W. S. Warren, E. Y. Chekmenev, Microtesla SABRE Enables 10% Nitrogen-15 Nuclear Spin Polarization, *Journal of the American Chemical Society* **137**, 1404 (2015).
94. T. Theis, G. X. Ortiz, Jr., A. W. J. Logan, K. E. Claytor, Y. Feng, W. P. Huhn, V. Blum, S. J. Malcolmson, E. Y. Chekmenev, Q. Wang, W. S. Warren, Direct and Cost-Efficient Hyperpolarization of Long-Lived Nuclear Spin States on Universal (15)N2-Diazirine Molecular Tags, *Science advances* **2**, e1501438 (2016).
95. M. H. Levitt, Singlet Nuclear Magnetic Resonance in *Annual Review of Physical Chemistry, Vol 63,* M. A. Johnson, T. J. Martinez, Eds. (2012), vol. 63, pp. 89-105.

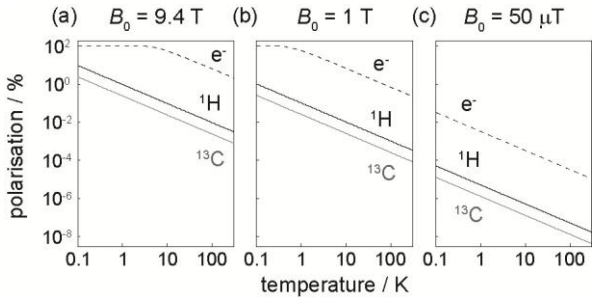

Figure 1. Polarisation level as a function temperature for ^{13}C nuclei (grey lines), ^{1}H nuclei (black lines) and unpaired electrons (dashed lines) with (a) B_0 = 9.4 T, (b) B_0 = 1 T, and (c) B_0 = 50 μT.

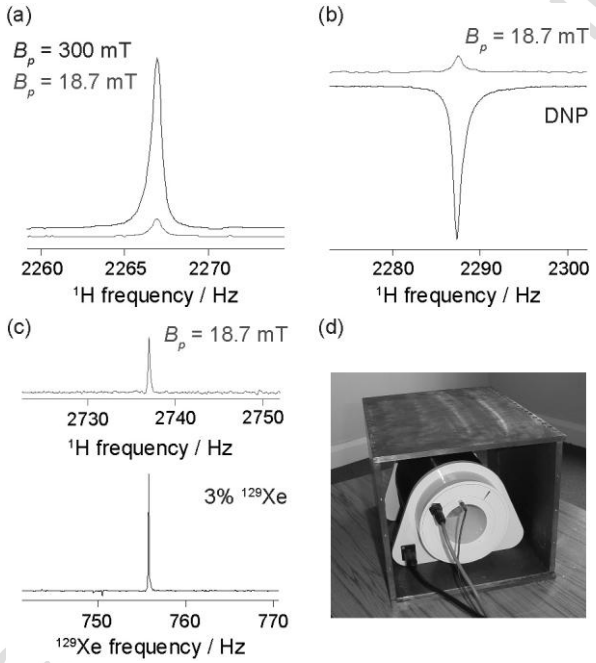

Figure 2. Hyperpolarisation enables the detection of ^{1}H and ^{129}Xe NMR spectra in the Earth's magnetic field. (a) Brute-force hyperpolarisation of 500 mL of water at B_p = 300 mT using a Halbach array (top, black), and at B_p = 18.7 mT using an electromagnet (bottom, grey). (b) 100 mL aqueous solution of 4-oxy-tempo hyperpolarised with brute-force at B_p = 18.7 mT (top, grey), and by Overhauser DNP at B_p = 2.5 mT (DNP irradiation at 124 MHz) (bottom, black). (c) ^{1}H EF NMR spectrum of toluene pre-polarised at B_p = 18.7 mT (top, grey), and a ^{129}Xe EF NMR spectrum of a 3% mixture of ^{129}Xe gas hyperpolarised to ~9% by stopped-flow SEOP (bottom). All spectra were acquired using the Terranova Earth's Field NMR device (Magritek Ltd, NZ) in (d). All data was taken from the PhD thesis of M. Halse.[45]

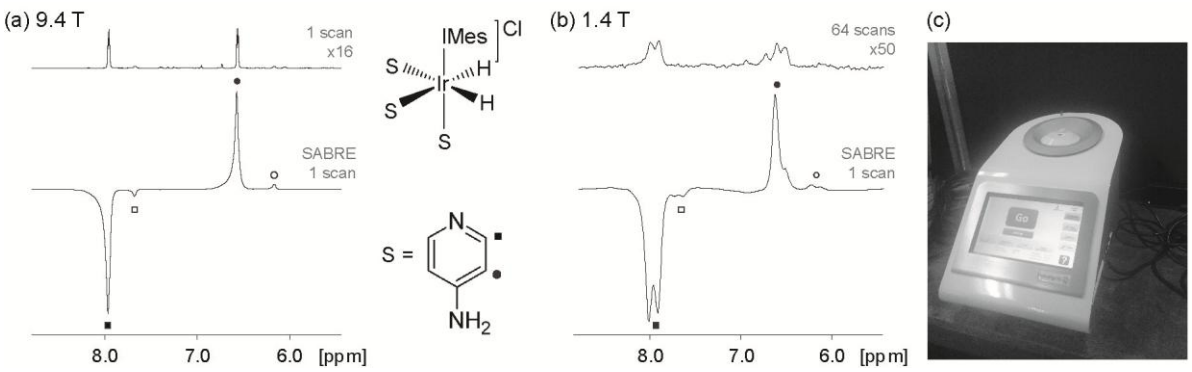

Figure 3. Thermally polarised (top, grey) and SABRE hyperpolarised (bottom, black) ^{1}H NMR spectra of 4-amino-pyridine acquired with (a) 400 MHz (Bruker AVIII, 9.4 T) and (b) 60 MHZ (1.4 T) NMR detection. (c) Photo of the 1.4 T compact NMR instrument (Nanalysis Corp., Canada). The sample was a 5 mm NMR tube containing 0.6 mL methanol-d_4, 2 mg (3.1 µmol) of the pre-catalyst Ir(IMes)(COD)(Cl), and 20 equivalents (5.8 mg) of the substrate (S = 4-amino-pyridine). The catalyst was activated to form $[Ir(H)_2(IMes)(S)_3]Cl$ by shaking the sample in the presence of a large excess of H_2.[79] For the SABRE experiments, the solution was put under 3 *atm* *p*-H_2 pressure, shaken for 8 s in the fringe field of the 400 MHz spectrometer (B < 10 G) and dropped into either the high-field (400 MHz) or low-field (60 MHz) NMR spectrometer for signal detection. Filled symbols highlight the *ortho* (squares) and *meta* (circles) proton peaks for the free substrate and open symbols denote substrate molecules bound to the iridium catalyst.

Table 1. Summary of the polarisation source and transfer mechanism for a range of NMR hyperpolarisation methods.

Hyperpolarisation method	Source of nuclear spin order	Polarisation transfer mechanism
Brute-force polarisation	Thermal polarisation in high polarisation field and/or at low temperature	N/A
Dynamic nuclear polarisation (DNP)	unpaired electron	Saturation of ESR transition; Overhauser effect, cross effect, solid effect and/or thermal mixing
Spin-exchange optical pumping (SEOP)	Optically pumped alkali metal vapour (e.g. Rb)	Spin-exchange collisions between noble gas nuclei (e.g. ^{3}He, ^{129}Xe, ^{83}Kr) and alkali metal
***Para*hydrogen-induced polarisation (PHIP)**	*para*hydrogen	Spin-conserved hydrogenation of an unsaturated substrate
Signal amplification by reversible exchange (SABRE)	*para*hydrogen	Exchange reaction involving *p*-H_2, catalyst and substrate; strong *J*-coupling mediated coherent transfer to substrate.
Chemically-induced DNP (CIDNP)	Spin correlated radical pair	Nuclear-spin-selective recombination of radical pair mediated by the hyperfine interaction.
Quantum-rotor-induced polarisation	Rotationally hindered methyl groups at liquid helium temperatures	Rapid sample dissolution; cross-relaxation via dipolar couplings